

The scintillating bar detector of the ASACUSA experiment

V. Mascagna,^{a,b,*} C. Amsler,^c M. Bayo,^{d,e} H. Breuker,^f M. Bumbar,^{g,h,i}
M. Cerwenka,^{c,g} G. Costantini,^{a,b} R. Ferragut,^{d,e} M. Giammarchi,^e
A. Gligorova,^j G. Gosta,^{a,b} H. Higaki,^k E. D. Hunter,^{h,i} C. Killian,^c
V. Kraxberger,^{c,g} N. Kuroda,^l M. Leali,^{a,b} G. Maero,^{e,m} C. Malbrunot,^{h,1}
Y. Matsuda,^l S. Migliorati,^{a,b} D. J. Murtagh,^c A. Nanda,^{c,g} L. Nowak,^{c,g}
M. Romé,^{e,m} M. C. Simon,^c M. Tajima,^{i,n} V. Toso,^{e,m} S. Ulmer,^f L. Venturelli,^{a,b}
A. Weiser,^{c,g} E. Widmann^c and Y. Yamazaki^f

^aDipartimento di Ingegneria dell'Informazione, Università degli Studi di Brescia, via Branze 38, Brescia, Italy

^bINFN Pavia, via Agostino Bassi, Pavia, Italy

^cStefan Meyer Institute, Austrian Academy of Science, Dominikanerbastei 16, Vienna, Austria

^dPolitecnico di Milano, Piazza Leonardo da Vinci 32, Milan, Italy

^eINFN Milano, Via Celoria 16, Milan, Italy

^fUlmer Fundamental Symmetries Laboratory, RIKEN, 2-1 Hirosawa, Wako, Saitama, Japan

^gVienna Doctoral School in Physics, University of Vienna, Boltzmanngasse 5, Vienna, Austria

^hExperimental Physics Department, CERN, Esplanade des Particules 1, Geneva, Switzerland

ⁱFaculty of Natural Sciences, Imperial College London, South Kensington Campus, London, UK

^jFaculty of Physics, University of Vienna, Boltzmanngasse 5, Vienna, Austria

^kGraduate School of Advanced Science and Engineering, Hiroshima University, 1-3-1 Kagamiyama, Higashi-Hiroshima, Hiroshima, Japan

^lInstitute of Physics, University of Tokyo, 7-3-1 Hongo, Bunkyo-ku, Tokyo, Japan

^mDipartimento di Fisica, Università degli Studi di Milano, Via Giovanni Celoria 16, Milan, Italy

ⁿJapan Synchrotron Radiation Research Institute, 1-1-1 Kouto, Sayo-cho, Sayo-gun, Hyogo, Japan

E-mail: valerio.mascagna@unibs.it

Detecting charged pions emitted from antiproton annihilation on nuclei is a well-established technique utilized to determine annihilation vertex positions, crucial for several experiments in the antimatter field. For the past decade, a detector composed of plastic scintillating bars has been integral to the ASACUSA experiment, employed in both antihydrogen formation experiments and annihilation cross-section measurements. This work outlines its design and operations, focusing on its role in these experimental applications.

EXA/LEAP2024,

26-30 August 2024

Austrian Academy of Sciences, Vienna, Austria

¹present address: TRIUMF, Vancouver, Canada

*Speaker

1. Introduction

The ASACUSA Collaboration at CERN’s Antiproton Decelerator has studied antihydrogen and hybrid atoms like antiprotonic helium for over 20 years to test fundamental symmetries and the matter-antimatter imbalance in the Universe [1–7]. Their research also includes antiproton collisions and annihilations on nuclei, primarily detected through pions emitted during these events [8–12].

For antihydrogen formation, antiprotons are slowed, trapped, and mixed with positrons, with pion detection helping locate the annihilation position. In collision experiments, antiprotons pass through thin material foils (from nm to μm scale), and annihilations are counted via pion detection. On average, these processes produce five pions, three of which are charged, with a mean momentum of approximately 200 MeV/c [13]. Charged pions are easily detectable using plastic scintillators and suitable light readout systems.

The collaboration employs a scintillating bar detector [14], which was crucial in demonstrating the first antihydrogen formation in a cusp trap [15]. In subsequent years, it has been used to monitor annihilations during trapping operations, providing a valuable tool for optimizing antihydrogen formation procedures [16–19].

2. The detector

The detector consists of scintillating bars arranged in $\sim 1\text{ m}^2$ panels placed around the interaction region, where antiprotons annihilate on nuclei. By detecting the emerging charged pions, the vertex position can be reconstructed. In Fig. 1 the setup used for the antihydrogen formation experiment is shown.

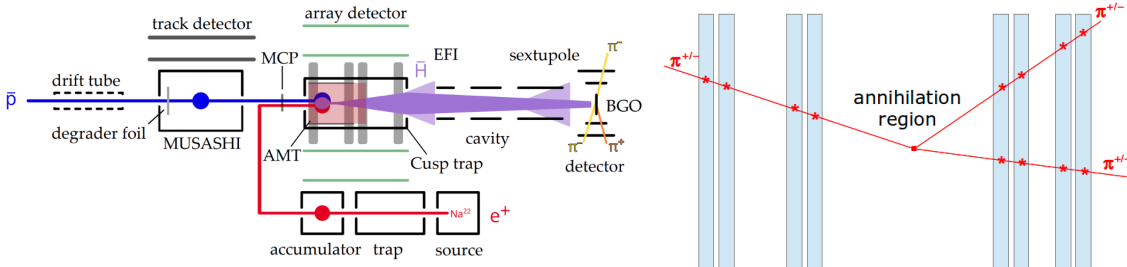


Figure 1: Left: sketch of antihydrogen formation experiment, where the scintillating bar panels (labeled as “array detector”) are placed close to the interaction region in a XY configuration (4 couples) to allow the 3D tracking of the charged pions emerging from the antiproton annihilations on the trap walls. Right: the annihilation position is reconstructed by detecting the pions on the scintillating bars and connecting their tracks back to a suitable unique origin.

The scintillating bars, produced through an extrusion process, are composed of Polystyrene Dow Styron 663W with 1% PPO + 0.03% POPOP, and are coated with a white TiO_2 layer [20]. Each bar (see Fig.2) has a cross-section of $1.5 \times 1.9\text{ cm}^2$ and a length of 96 cm. A 2 mm central groove houses a 1 mm diameter Y-11 wavelength shifting (WLS) fiber from Kuraray [21]. The fibers are individually darkened, cut, polished, and coupled to a Silicon Photomultiplier (SiPM) using a custom 3D-printed connector [22].

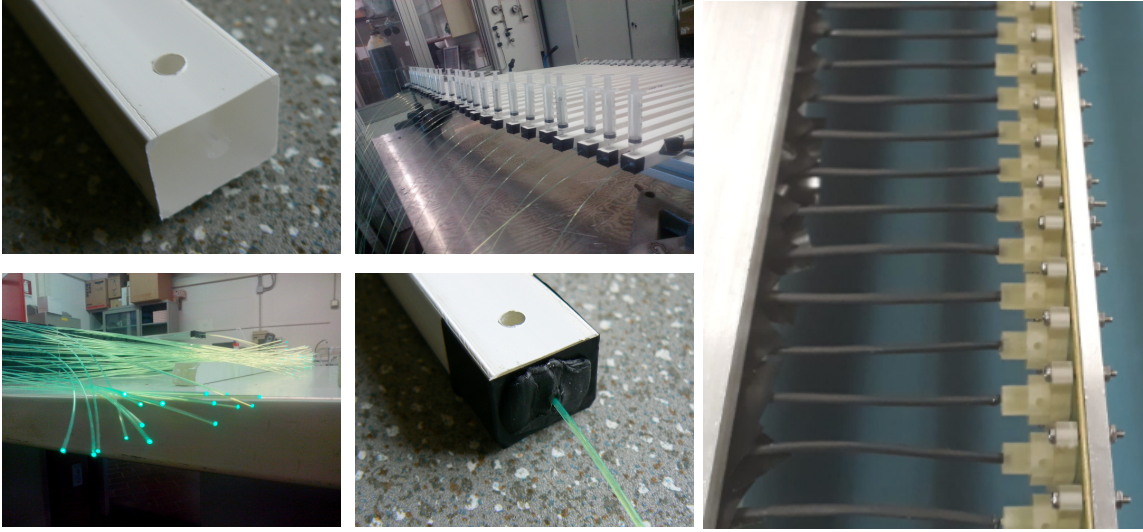


Figure 2: Photograph showing the scintillating bars at various stages of detector assembly: fiber preparation and gluing inside the bars are depicted on the left, while the darkened fibers connected to the 3D-printed connector and SiPMs are also shown on the right.

The SiPM model is the ASD RGB-SiPM by AdvanSiD [23], featuring a $1 \times 1 \text{ mm}^2$ active area with 625 cells ($40 \mu\text{m}$ pitch). Encapsulated in a $2.02 \times 2.48 \times 1.30 \text{ mm}^3$ SMD plastic package with a transparent epoxy layer, it was chosen for its efficient absorption spectrum (peaking at 550 nm) matching the green WLS fibers' emission, as well as its intrinsic radiation hardness [24].

The SiPM readout board is shown in Fig. 3: each board hosts 12 surface-mounted SiPMs, with five boards required to read out the 60 SiPMs in each panel. These boards are mounted close to the scintillating bars on the internal frame. Each channel features a dual AD8002 current feedback amplifier and the necessary passive components, with a footprint matching the bar cross-section. The signals are transmitted to the Front-End Board (FEB) via $\sim 50 \text{ cm}$ Hirose U.FL series thin coaxial cables [25] and connect to the 8×8 multi-anode PMT socket on the main FEB. A PMT-dedicated board was used for the SiPM readout to leverage the existing front-end board from the previous detector version, which employed multi-anode PMTs for light readout (all the details concerning the upgrade are described in [14]).

The readout of each SiPM signal is managed by a FEB which is based on the MAROC3 (Multi-Anode ReadOut Chip 3) ASIC, developed by the Omega group at LAL [26]. The board integrates the MAROC3 chip along with two ALTERA Cyclone II FPGAs (model EP2C8Q208I8N, Altera Corporation) for configuration and data readout, and a 12-bit analog-to-digital converter (ADC) circuit (model AD9220ARZ, Analog Devices [27]). The MAROC board, shown on the right in Fig. 3, also supplies power to the components and includes all necessary connectors for VME electronics communication (analog and digital I/O, trigger signals) and a 64-pin socket for analog input signals.

The MAROC3 chip hosted on the board is a 64-channel front-end circuit designed for PMT or SiPM signal readout. It provides a single shaped signal proportional to the input charge and 64 digital trigger outputs [26]. Each input channel features a variable-gain preamplifier with 8-bit tunable gain (up to a factor of 4) and low input impedance. A current mirror splits the signal into

two separate processing paths, each serving a distinct purpose with different timing characteristics:

- **Analog Path** (hundreds of ns time scale): this path is optimized for acquiring and digitizing the peak amplitude of the input signal, preserving information about the original light pulse produced in the scintillating bar. It consists of an RC buffer, a slow tunable shaper, and two sample-and-hold circuits for measuring the signal amplitude and baseline. The slow shaper feedback capacitors (300, 600 and 1200 fF) can be independently configured via three switches to shape the signal with different widths and peak time. Moreover, the input signal gain in the shaper can be fine tuned by adjusting four capacitors in the RC buffer, optimizing the signal-to-noise ratio. A 5 MHz clock multiplexer is also included for synchronization.
- **Digital Path** (tens of ns time scale): this path is designed for fast signal processing to generate a rapid trigger. It includes a fast shaper and a discriminator with a tunable threshold. If the signal exceeds this threshold, a digital pulse is generated and sent to the acquisition system where all the signal sources are combined with the desired logic to form the system trigger. With a shaping time in the range of tens of nanoseconds, this path enables self-triggering and can also be used for counting purposes.

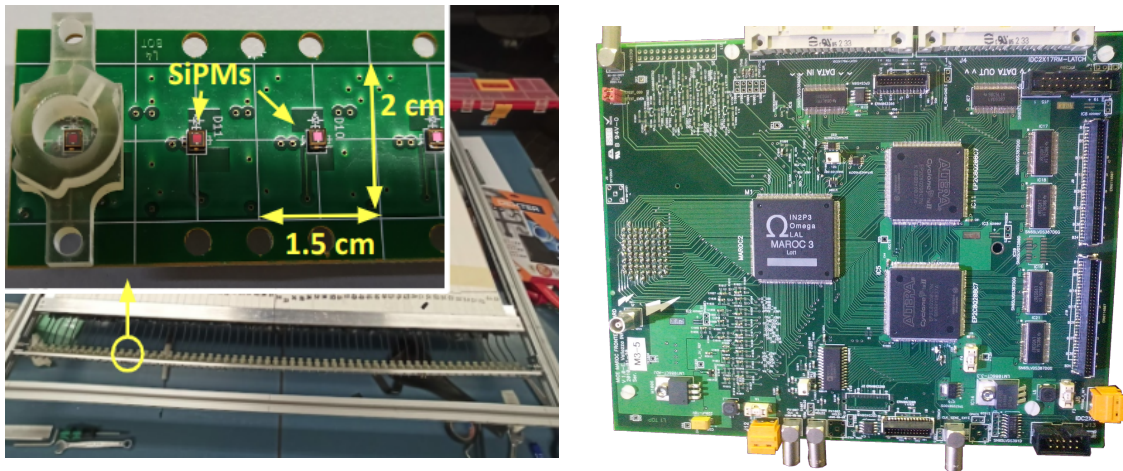


Figure 3: The amplifier board with the surface-mounted SiPM is shown on the left; the Maroc3 based front-end board is shown on the right.

All MAROC3 parameters were optimized through extensive laboratory testing, as detailed in [14]. These tests also provided insights into the detector’s performance, revealing a spatial resolution of ~ 6 mm for a pion hit on a single plane, with an efficiency of about 90%. Regarding the resolution of the annihilation vertex position, an estimate obtained during the calibration at the start of each antihydrogen experiment data-taking session yielded a value of a few cm. This relatively low resolution is primarily attributed to multiple scattering through the cusp trap material and misalignment of the detector panels.

3. Application in antihydrogen experiments

The most straightforward process to measure the vertex of antiprotons annihilating on nuclei, a process which typically produces 3 charged pions, is to detect the pions and trace them back to the annihilation position.

In the anti-hydrogen experiment of the ASACUSA collaboration the detector is operated in self-trigger mode and the scintillating bar panels are placed close to the cusp trap so that it can detect emerging pions with a solid angle coverage of $\sim 10\text{--}15\%$ depending on the setup (see Fig. 1).

All trapping operations are monitored using several detectors, including the scintillating bar detector, which provides two main types of data to the experiment:

- Hit counts: triggers, generated from the discriminated pulses of each bar as described in the “digital path” in Sec.2, are sent to an acquisition board directly connected to the main cusp trap control system;
- annihilation vertex position and time: signals from the “analog path” of the MAROC3 chip are processed to determine the amplitude of each bar signal. These signals are then used to reconstruct the annihilation position and time (an example plot generated during a trapping cycle is shown in Fig. 4).

The data provided by the detector is utilized both to fine-tune the trap parameters on a shot-by-shot basis during the development phases and, later, to perform more quantitative analyses after a data-taking period has concluded.

In Fig. 4 an example of the provided data is shown.

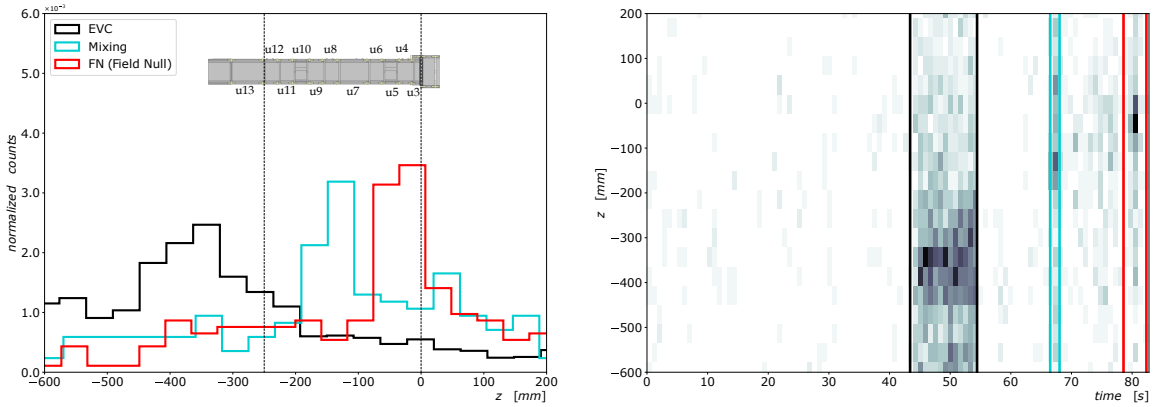


Figure 4: A typical monitoring plot generated after a single trapping cycle (Figure from [28]). The annihilation counts are displayed as a function of position along the beam axis (z), which extends from negative to positive values (left), and as a function of z vs. time (right). Different colors indicate various trap operations: evaporative cooling (EVC), mixing with positrons, or dumping antiprotons into the downstream field null (FN) region at $z \approx 0$ mm. The cusp electrode layout is superimposed on the figure.

4. Conclusions

The scintillating bar detector has proven to be a useful tool for the ASACUSA experiment, effectively enabling the detection of charged pions and reconstruction of annihilation vertices. Its

design, featuring extruded plastic scintillators coupled with SiPMs and MAROC3-based front-end electronics, has demonstrated adaptability across various experimental setups, including antihydrogen formation and annihilation cross-section measurements. The detector's ability to provide both spatial and temporal information has been important in optimizing trapping operations and improving the overall experimental efficiency.

References

- [1] Y. Enomoto, N. Kuroda, K. Michishio, C.H. Kim, H. Higaki, Y. Nagata et al., *Synthesis of cold antihydrogen in a cusp trap*, *Phys. Rev. Lett.* **105** (2010) 243401.
- [2] N. Kuroda, S. Ulmer, D.J. Murtagh, S. Van Gorp, Y. Nagata, M. Diermaier et al., *A source of antihydrogen for in-flight hyperfine spectroscopy*, *Nature Communications* **5** (2014) 3089.
- [3] C. Malbrunot, C. Amsler, S. Arguedas Cuendis, H. Breuker, P. Dupre, M. Fleck et al., *The asacusa antihydrogen and hydrogen program: results and prospects*, *Philosophical Transactions of the Royal Society A: Mathematical, Physical and Engineering Sciences* **376** (2018) 20170273.
- [4] B. Kolbinger, C. Amsler, S.A. Cuendis, H. Breuker, A. Capon, G. Costantini et al., *Measurement of the principal quantum number distribution in a beam of antihydrogen atoms*, *The European Physical Journal D* **75** (2021) 91.
- [5] M. Hori, A. Sótér, D. Barna, A. Dax, R. Hayano, S. Friedreich et al., *Two-photon laser spectroscopy of antiprotonic helium and the antiproton-to-electron mass ratio*, *Nature* **475** (2011) 484.
- [6] M. Hori, H. Aghai-Khozani, A. Sótér, D. Barna, A. Dax, R. Hayano et al., *Buffer-gas cooling of antiprotonic helium to 1.5 to 1.7 k, and antiproton-to-electron mass ratio*, *Science* **354** (2016) 610.
- [7] A. Sótér, H. Aghai-Khozani, D. Barna, A. Dax, L. Venturelli and M. Hori, *High-resolution laser resonances of antiprotonic helium in superfluid 4He* , *Nature* **603** (2022) 411.
- [8] H. Aghai-Khozani, D. Barna, M. Corradini, R. Hayano, M. Hori, T. Kobayashi et al., *First experimental detection of antiproton in-flight annihilation on nuclei at ~ 130 keV*, *The European Physical Journal Plus* **127** (2012) 125.
- [9] H. Aghai-Khozani, D. Barna, M. Corradini, D. De Salvador, R. Hayano, M. Hori et al., *First measurement of the antiproton-nucleus annihilation cross section at 125 keV*, *Hyperfine Interactions* **234** (2015) 85.
- [10] K. Todoroki, D. Barna, R. Hayano, H. Aghai-Khozani, A. Sótér, M. Corradini et al., *Instrumentation for measurement of in-flight annihilations of 130 keV antiprotons on thin target foils*, *Nuclear Instruments and Methods in Physics Research Section A: Accelerators, Spectrometers, Detectors and Associated Equipment* **835** (2016) 110.

- [11] H. Aghai-Khozani, A. Bianconi, M. Corradini, R. Hayano, M. Hori, M. Leali et al., *Measurement of the antiproton–nucleus annihilation cross-section at low energy*, *Nuclear Physics A* **970** (2018) 366.
- [12] H. Aghai-Khozani, D. Barna, M. Corradini, D. De Salvador, R. Hayano, M. Hori et al., *Limits on antiproton-nuclei annihilation cross sections at ~ 125 keV*, *Nuclear Physics A* **1009** (2021) 122170.
- [13] G. Bendiscioli and D. Kharzeev, *Antinucleon-nucleon and antinucleon-nucleus interaction. a review of experimental data*, *La Rivista del Nuovo Cimento (1978-1999)* **17** (2007) 1.
- [14] G. Costantini, L. Giorleo, G. Gosta, M. Leali, V. Mascagna, S. Migliorati et al., *The upgrade of the asacusa scintillating bar detector for antiproton annihilation measurements*, *Journal of Instrumentation* **18** (2023) P04013.
- [15] Y. Enomoto, N. Kuroda, K. Michishio, C.H. Kim, H. Higaki, Y. Nagata et al., *Synthesis of cold antihydrogen in a cusp trap*, *Phys. Rev. Lett.* **105** (2010) 243401.
- [16] Y. Nagata, N. Kuroda, M. Ohtsuka, M. Leali, E. Lodi-Rizzini, V. Mascagna et al., *Direct detection of antihydrogen atoms using a bgo crystal*, *Nuclear Instruments and Methods in Physics Research Section A: Accelerators, Spectrometers, Detectors and Associated Equipment* **840** (2016) 153.
- [17] C. Sauerzopf, A.A. Capon, M. Diermaier, P. Dupré, Y. Higashi, C. Kaga et al., *Towards measuring the ground state hyperfine splitting of antihydrogen – a progress report*, *Hyperfine Interactions* **237** (2016) 103.
- [18] B. Kolbinger, C. Amsler, H. Breuker, M. Diermaier, P. Dupré, M. Fleck et al., *Recent developments from asacusa on antihydrogen detection*, *EPJ Web of Conferences* **181** (2018) .
- [19] E. Widmann, C. Amsler, S. Arguedas Cuendis, H. Breuker, M. Diermaier, P. Dupré et al., *Hyperfine spectroscopy of hydrogen and antihydrogen in asacusa*, *Hyperfine Interactions* **240** (2018) 5.
- [20] A. Pla-Dalmau, A.D. Bross and K.L. Mellott, *Low-cost extruded plastic scintillator*, *Nuclear Instruments and Methods in Physics Research Section A: Accelerators, Spectrometers, Detectors and Associated Equipment* **466** (2001) 482.
- [21] Kuraray, “Scintillating fibers and wavelength shifting fibers.”
https://www.kuraray.com/uploads/5a717515df6f5/PR0150_psf01.pdf.
- [22] G. Costantini, L. Giorleo, G. Gosta, M. Leali, V. Mascagna, S. Migliorati et al., *Upgrade of the scintillating bars detector for the asacusa experiment*, *EPJ Web Conf.* **262** (2022) 01013.
- [23] AdvanSiD, “Rbg sipms - chip scale package (csp).”
https://indico.cern.ch/event/566138/contributions/2287560/attachments/1400219/2139199/Advansid_datasheet_RGB.pdf.

- [24] F. Acerbi, G. Ballerini, A. Berra, C. Brizzolari, G. Brunetti, M. Catanesi et al., *Irradiation and performance of RGB-HD silicon photomultipliers for calorimetric applications*, *Journal of Instrumentation* **14** (2019) P02029.
- [25] Hirose Electric, “U.fl series.” <https://www.hirose.com/product/series/U.FL>.
- [26] S. Blin, P. Barrillon and C. de La Taille, *Maroc, a generic photomultiplier readout chip*, *Journal of Instrumentation* **5** (2010) C12007.
- [27] Analog Devices, “Ad9220.” <https://www.analog.com/en/products/ad9220.html>.
- [28] ASACUSA collaboration, *STATUS REPORT OF THE AD-3 ASACUSA COLLABORATION*, Tech. Rep. CERN-SPSC-2024-007, SPSC-SR-342, CERN, Geneva (2024).